Amortized Variational Inference for Road Friction Estimation

Shuangshuang Chen*[1,2], Sihao Ding[2], L. Srikar Muppirisetty[2], Yiannis Karayiannidis[3], Mårten Björkman[1]

***Abstract*— Road friction estimation concerns inference of the coefficient between the tire and road surface to facilitate active safety features. Current state-of-the-art methods lack generalization capability to cope with different tire characteristics and models are restricted when using Bayesian inference in estimation while recent supervised learning methods lack uncertainty prediction on estimates. This paper introduces variational inference to approximate intractable posterior of friction estimate and learns amortized variational inference model from tire measurement data to facilitate probabilistic estimation while sustaining the flexibility of tire models. As a by-product, a probabilistic tire model can be learned jointly with friction estimator model. Experiments on simulated and field test data show that the learned friction estimator provides accurate estimates with robust uncertainty measure in a wide range of tire excitation levels. Meanwhile, the learned tire model reflects well-studied tire characteristics from field test data.**

I. Introduction

The Tire-Road friction coefficient, commonly referred to as road friction, is defined by the maximum ratio between horizontal and nominal tire forces in the tire coordinate system [1]. Applications of friction coefficient on Advanced Driver Assistant System (ADAS) and Autonomous Driving (AD) to better control vehicle responses has been proposed such in Adaptive Cruise Control [2], Autonomous Emergency Braking [3] and Electronic Stability Control [4]. The significance on accurate and real-time road friction estimation has been addressed in both research community and industry over the last few decades [1], [5]–[8]. Gustafsson in [5] utilizes sensitive indication of friction from longitudinal stiffness at low tire excitation. Svendenius in [7] utilizes longitudinal slip and force to estimate friction at higher excitation. Nevertheless, these vehicle dynamics-based methods only performs with acceptable accuracy in a narrow estimation range and significant excitation of tires is required for high estimation accuracy for most of methods [9]. Furthermore, the tractability of Bayesian inference in estimation restricts tire and vehicle models to be simple to further impedes accurate estimation by using more flexible tire model. To sustain the estimation performance at most of tire excitation levels, [8] proposes to fuse estimates from multiple individual estimation module using different tire characteristics. However, it is difficult to generalize the method to all types of tires and surfaces and requires significant efforts to model and tune.

Due to the limitations in estimation algorithms in Bayesian framework, recent works resort to pure data-driven methods using supervised learning techniques to model complicated relations between tire, vehicle states and friction coefficient, while others leverage other information resources e.g. road unevenness [10], [11], video sequences of road segments [12], weather information [13] to extract friction coefficient. Such formulations have three main disadvantages: overfitting brought by supervised learning degrades the performance of estimator in practice; point estimates without uncertainty measure makes it impossible to scrutinize wrong estimates which possibly leads to serious consequences like road accidents; indirect indication of friction coefficient from such as road unevenness, pixels of road segments only reveals partial causal relation without considering tire involvement.

To better extract tire-road friction information, we consider tire as a probe sensor and estimate the coefficient by tire response. In order to remove the restriction in modeling by Naïve Bayesian inference, we propose variational inference to approximate the intractable estimation, and the amortized variational model could be learned in advance from tire measurement data and applied in real-time. The main contributions of this paper are:

- The proposed data-driven approach facilitates the estimation algorithm to infer friction regardless of tire characteristics and excitation levels, without labors on hand-craft algorithms and tuning;
- The friction estimator alleviates the restriction in complexity of tire modeling and utilizes tire forces and moments collectively to extract hidden information on friction with greater accuracy and confidence;
- The friction estimator keeps the merit of Bayesian framework to infer the distribution of estimates, allowing low-confidence estimates to be scrutinized and to apply on e.g. conservative or aggressive control strategies according to use cases;
- The learned tire model, as an by-product, illustrating well-studied tire characteristics provides an alternative tool in accurate tire modelling for simulation and tire characteristics studies.

We present the paper as follows: Section II formulates friction estimation as a Bayesian inference and clarifies the fundamental difficulties of naïve approach; Section III introduces amortized variational inference model for friction

*Corresponding Author
[1]Division of Robotics, Perception, Learning, Royal Institute of Technology, 100 44 Stockholm, Sweden, {shuche, celle}@kth.se
[2]Volvo Car Corporation, {chen.shuangshuang, sihao.ding, srikar.muppirisetty}@volvocars.com
[3]Department of Electrical Engineering, Chalmers University of Technology, 412 96 Gothenburg, Sweden, yiannis@chalmers.se

estimation and model tire as a generative model, and describes how these models are learned from data; Section IV demonstrates the validity of the proposed method on simulated and field test data.

II. Friction Estimation as Bayesian Inference

In most of well-studied analytic and empirical steady-state tire models such as *Brush* model, *Dugoff* model, *Magic Formula* [14], *MF-Tyre* [15], friction coefficient is a determinant factor. As shown in Fig. 1a, friction coefficient (i.e. typical dry and icy road surface) not only affects lateral force maximum, but also the combined slip effects. The same observations could be found in longitudinal force and other tire moments [15], as Fig. 1b shows the combined slip effect on dried surface in detail as Fig. 1a. Therefore, more accurate estimates are expected when using forces and moments altogether. Considering friction coefficient μ and

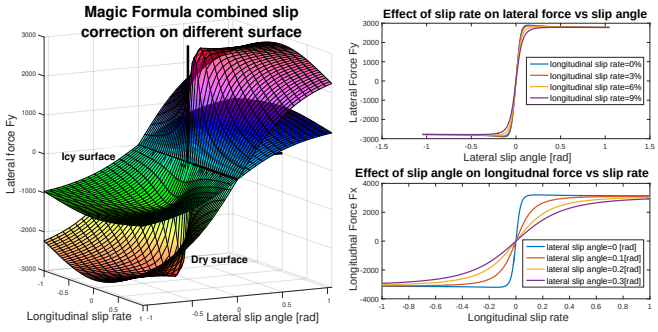

(a) Lateral force with combined slip on different road surface (b) Combined longitudinal and lateral slip effect on tire forces

Fig. 1: Combined slip correction on tire forces of *Magic Formula on varied road surfaces.*

tire state variables, tire model reveals their relations to tire forces and moments, $\mathbf{F}$, in terms of a function $\mathbf{T}(\mu, \cdot)$. To keep the formulation intact, we leave all tire state variables as $(\cdot)$. It can be defined according to the complexity of tire models, which commonly includes longitudinal slip and lateral slip, inclination angle and etc. Given tire forces and state variables, friction coefficient estimation can be viewed as a Bayesian inference problem to compute the conditional posterior $p(\mu|\mathbf{F}, \cdot)$ using Bayes rule [6]:

$$p(\mu|\mathbf{F}, \cdot) = \frac{p(\mathbf{F}|\mu, \cdot)p(\mu)}{\int p(\mathbf{F}|\mu, \cdot)p(\mu)\mathrm{d}\mu} = \frac{p(\mathbf{F}|\mathbf{T}(\mu, \cdot))p(\mu)}{\int p(\mathbf{F}|\mathbf{T}(\mu, \cdot))p(\mu)\mathrm{d}\mu}, \tag{1}$$

where $p(\mathbf{F}|\mu, \cdot)$ is conditional likelihood of $\mathbf{F}$ given μ and $p(\mu)$ is prior of friction coefficient. However, the exact estimation by eq.(1) is commonly impossible at all tire performance ranges in practice. It is tractable unless when prior is a Gaussian distribution and tire model $\mathbf{T}(\mu, \cdot)$ is a linear function of μ, which is contradictory to the nonlinearity of tire models in larger slip regions [16]. There are two trendy solutions, however, leading to new issues.

A common practice is to approximate the integral in eq.(1) by summation, by replacing the continuous variable μ with a pre-defined set of J discrete hypotheses $\mathcal{U} = \{\mathcal{U}_1, \mathcal{U}_2, \ldots, \mathcal{U}_j, \ldots, \mathcal{U}_J\}$ [6]. Thus, the intractable posterior is simplified as:

$$P(\mu = \mathcal{U}_j|\mathbf{F}, \cdot) = \frac{P(\mathbf{F}|\mu = \mathcal{U}_j, \cdot)P(\mu = \mathcal{U}_J)}{\sum_i P(\mathbf{F}|\mu = \mathcal{U}_i, \cdot)P(\mu = \mathcal{U}_i)}. \tag{2}$$

A critical difficulty brought by this approximation is the interpretation of the posterior $p(\mu = \mathcal{U}_j|\mathbf{F}, \cdot)$. $p(\mu = \mathcal{U}_i|\mathbf{F}, \cdot)$ is a cumulative probability instead of a probability density at $\mathcal{U}_i$. Nevertheless, the unspecified intervals of the cumulative probability is impossible to properly defined, which makes it difficult for later decision making algorithm design.

The another option is to approximate nonlinear tire model $\mathbf{T}(\mu, \cdot)$ by piece-wise linear function to ensure estimation is exact locally [9]. The exact estimate is computed for each specific performance region and integration rule fuses all estimates. To compensate model inaccuracy, [8] proposes to fuse estimates from multiple estimate algorithms according to different tire characteristics. However, this approximation increases computational cost if tire model needs complex combination of multiple functions which might makes it impossible in real time. Secondly, due to complication of behavior in different types of tire, this methods requires substantial experiments in designing estimation and fusion algorithm, limiting its applicability to general types of tires.

We know that the combined slip effect of tire leads to more accurate and confident estimation of friction, however, exact inference is impossible in practice. To keep the inference tractable, but maintain the flexibility of tire models, we leverage approximation of exact inference. Although exact inference is of interest, approximate inference is adequate for decision making i.e. determining speed or activating ADAS functions accordingly. There are two main categories of approximation methods for Bayesian inference: deterministic approximations, such as variational Bayes and expectation propagation, and stochastic approximation such as Monte Carlo methods. In general, Monte Carlo methods require a sufficiently large sample size for unbiased estimation, which is not perferable for real-time estimation. On the other hand, variational inference uses a variational distribution $q(\mu|\mathbf{F}, \cdot)$ from a tractable family $\mathcal{Q}$ to approximate true posterior [17]. We will discuss variational inference for friction estimation in detail in next section.

III. Amortized Variational Inference for Friction Estimation

Variational inference is to use a variational distribution $q(\mu|\mathbf{F}, \cdot)$ as approximation of true posterior $p(\mu|\mathbf{F}, \cdot)$ from a tractable family $\mathcal{Q}$. The optimal variational distribution $q^*(\mu|\mathbf{F}, \cdot)$ is obtained when KL divergence between the variational distribution $q(\mu|\mathbf{F}, \cdot)$ and true posterior $p(\mu|\mathbf{F}, \cdot)$ is minimized to zero. Nevertheless, true posterior is unknown therefore to be approximated, so direct minimization of KL divergence is not possible. Instead of minimizing KL divergence, variational inference solves the dual problem of

it by maximizing the lower bound of marginal likelihood of observable variables. As seen in previous section, the observable variables are forces and moments measurements, $\mathbf{F}$. The log-marginal likelihood $p(\mathbf{F}|\cdot)$ of it could be decomposed into two parts:

$$\begin{aligned}\log p(\mathbf{F}|\cdot) &= \log \int p(\mathbf{F}|\mu,\cdot)p(\mu)d\mu \\ &= \mathcal{L} + \mathrm{KL}(q(\mu|\mathbf{F},\cdot)||p(\mu|\mathbf{F},\cdot)),\end{aligned} \tag{3}$$

where $\mathrm{KL}(q_{\boldsymbol{\phi}}(\mu|\mathbf{F},\cdot)||p(\mu|\mathbf{F},\cdot))$ is the KL divergence between the variational and true posterior, and $\mathcal{L}$, also called the Evidence Lower Bound (ELBO). Therefore, minimizing the second term is equivalent to maximizing $\mathcal{L}$ since $\log p(\mathbf{F}|\cdot)$ is a constant. Instead of online optimization on each new data points, we use amortized variational inference by specifying a set of parameters, $\boldsymbol{\phi}$, to model variational distribution. The joint likelihood $p(\mathbf{F},\mu|\cdot)$ could be considered as a generative model with conditional likelihood $p(\mathbf{F}|\mathbf{T}(\mu,\cdot))$ and prior $p(\mu)$ of a latent variable μ. We also parameterize the generative model by a set of parameters, $\boldsymbol{\theta}$. To be noted, $p_{\boldsymbol{\theta}}(\mathbf{F}|\mu,\cdot)$ could be given by any analytic or fitted empirical tire models or learned from data. Using parameterization on variational posterior and generative model, $\mathcal{L}$ is composed of two terms:

$$\mathcal{L} = \mathbb{E}_{q_{\boldsymbol{\phi}}(\mu|\mathbf{F},\cdot)} \log p_{\boldsymbol{\theta}}(\mathbf{F}|\mu,\cdot) - \mathrm{KL}(q_{\boldsymbol{\phi}}(\mu|\mathbf{F},\cdot)||p(\mu)), \tag{4}$$

The first term is the expectation of the conditional distribution over the variational posterior; the second term is the KL divergence between variational posterior and prior. In principal, the variational posterior $q_{\boldsymbol{\phi}}(\mu|\mathbf{F},\cdot)$, conditional likelihood $p_{\boldsymbol{\theta}}(\mathbf{F}|\mu,\cdot)$ and prior $p(\mu)$ could be chosen from any distribution family as long as ELBO could be computed analytically or easy to estimate. For convenience, we specify the variational posterior $q_{\boldsymbol{\phi}}(\mu|\mathbf{F},\cdot)$ and prior $p(\mu)$ as Gaussian distributions, so that the KL divergence term in eq.(4) has an analytical solution [18]. Similarly, the conditional likelihood $p_{\boldsymbol{\theta}}(\mathbf{F}|\mu,\cdot)$ is specified as a Gaussian distribution with a diagonal covariance matrix to simplify the model. Both parameters $\boldsymbol{\theta}$ and $\boldsymbol{\phi}$ are modelled by multi-layer neural networks (MLP). In summary,

$$\begin{aligned}\mathbf{F} &\sim p_{\boldsymbol{\theta}}(\mathbf{F}|\mu,\cdot) = \mathcal{N}(\boldsymbol{v}_{\boldsymbol{\theta}}(\mu,\cdot), \mathrm{diag}(\boldsymbol{\sigma}^2_{\boldsymbol{\theta}}(\mu,\cdot))) \\ \mu &\sim q_{\boldsymbol{\phi}}(\mu|\mathbf{F},\cdot) = \mathcal{N}(v_{\boldsymbol{\phi}}(\mathbf{F},\cdot), \sigma^2_{\boldsymbol{\phi}}(\mathbf{F},\cdot)),\end{aligned} \tag{5}$$

where $\boldsymbol{v}_{\boldsymbol{\theta}}(\mu,\cdot)$ and $\boldsymbol{\sigma}^2_{\boldsymbol{\theta}}(\mu,\cdot)$ are the mean and variance of the conditional likelihood of $\mathbf{F}$, while $v_{\boldsymbol{\phi}}(\mathbf{F},\cdot)$ and $\sigma^2_{\boldsymbol{\phi}}(\mathbf{F},\cdot)$ are the mean and variance of the variational posterior of μ respectively. With a non-informative Gaussian prior, the inferred latent variable μ might not directly correspond to the actual meaningful friction coefficient, which would require to learn an extra mapping between the coefficient and inferred latent variable. To avoid it, we use an informative Gaussian prior during training instead. Similar to the semi-supervised learning setup in [18], a part of training data has prior $\mathcal{N}(\mu_{GT}, \sigma^2)$ with mean as the ground truth μ_{GT} and variance σ^2 as the function of tire state variables $\sigma^2(\cdot)$ to account for data inaccuracy.

The expectation term in eq.(4) can then be estimated using reparameterization trick [19]:

$$\begin{aligned}&\mathbb{E}_{q_{\boldsymbol{\phi}}(\mu|\mathbf{F},\cdot)} \log p_{\boldsymbol{\theta}}(\mathbf{F}|\mu,\cdot) = \mathbb{E}_{\mathcal{N}(\epsilon;0,1)} \log p_{\boldsymbol{\theta}}(\mathbf{F}|\tilde{\mu},\cdot) \\ &\tilde{\mu} = v_{\boldsymbol{\phi}}(\mathbf{F},\cdot) + \sigma^2_{\boldsymbol{\phi}}(\mathbf{F},\cdot)\epsilon \qquad \epsilon \sim \mathcal{N}(0,1),\end{aligned} \tag{6}$$

where $\tilde{\mu}$ is sampled from variational posterior $q_{\boldsymbol{\phi}}(\mu|\mathbf{F},\cdot)$ and ϵ is a random variable sampled from Gaussian. Reparameterization trick allows for automatic differentiation to optimize $\boldsymbol{\theta}$ and $\boldsymbol{\phi}$ using auxiliary random variable ϵ to avoid stochastic variable $\tilde{\mu}$ blocking the differentiation chain, and decreases variance of estimates. Fig. 2 illustrates the amortized variational friction estimator $q_{\boldsymbol{\phi}}(\mu|\mathbf{F},\cdot)$ and probabilistic tire model $p_{\boldsymbol{\theta}}(\mathbf{F}|\mu,\cdot)$.

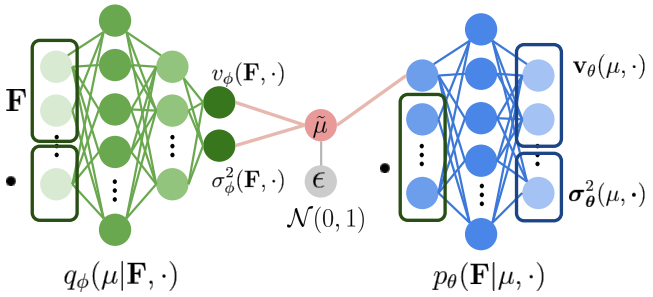

Fig. 2: Neural network topology of the probabilistic tire model $p_{\boldsymbol{\theta}}(\mathbf{F}|\mu,\cdot)$ and variational friction coefficient estimator $q_{\boldsymbol{\phi}}(\mu|\mathbf{F},\cdot)$. The reparameterization trick [19] enables automatic differentiation with $\tilde{\mu}$ sampled from $q_{\boldsymbol{\phi}}(\mu|\mathbf{F},\cdot)$.

The optimization of ELBO w.r.t. $\boldsymbol{\theta}$ and $\boldsymbol{\phi}$ is done jointly by *stochastic gradient variational Bayes* [19], using unbiased estimates of gradients:

$$\begin{aligned}\nabla_{\boldsymbol{\theta},\boldsymbol{\phi}}\mathcal{L} = \mathbb{E}_{\mathcal{N}(\epsilon|0,1)}[\nabla_{\boldsymbol{\theta},\boldsymbol{\phi}} \log p_{\boldsymbol{\theta}}(\mathbf{F}|v_{\boldsymbol{\phi}}(\mathbf{F},\cdot) + \sigma^2_{\boldsymbol{\phi}}(\mathbf{F},\cdot)\epsilon)] \\ - \nabla_{\boldsymbol{\theta},\boldsymbol{\phi}}\mathrm{KL}(q_{\boldsymbol{\phi}}(\mu|\mathbf{F},\cdot)||p(\mu)).\end{aligned}$$

IV. Experiments

To prove the validity of the proposed method, we evaluate learned variational friction estimator $q_{\boldsymbol{\phi}}(\mu|\mathbf{F},\cdot)$ and probabilistic tire model $p_{\boldsymbol{\theta}}(\mathbf{F}|\mu,\cdot)$ on both simulated and tire trailer field test data. In order not to introduce additional heuristics, we only select the most dominant tire states including longitudinal slip s, lateral slip α and nominal tire force F_z, and force vector $\mathbf{F}$ including longitudinal and lateral tire forces F_x, F_y.

A. Simulation experiments

As opposed to [20] that simulates tire states directly from *MF-Tyre*, we set up different driving maneuvers and road profiles in *IPG CarMaker*® to create a more realistic dataset. Compared to [20], simulated data here is unbalanced in longitudinal and lateral excitation levels which makes learning harder, but evaluation closer to reality.

1) Scenarios and maneuvers: CarMaker simulations run on different handling maneuvers and road profiles setups. Table I lists all definitions of used maneuvers, their covering ranges of longitudinal and lateral slip and variants in defined

maneuvers. These maneuvers, corresponding to various tire responses under realistic driving, are to better understand the generalization of learned friction estimator and probabilistic tire model on different slip ranges especially for unseen scenarios. Some in Table I are defined similarly as [21], while others are commonly used in testing and verification purpose for vehicle dynamics. Road surfaces are defined by patches of 10 discrete friction coefficient from 0.1 to 1.0. The tire models used in simulations are 245_35/R19 for front and 295_35/R19 for rear tire.

TABLE I: Handling maneuvers for data generation in CarMaker

Maneuver	Longitudinal slip range	Lateral slip range	Variants in maneuvers
B/A [a]	M $\sim$ H	L $\sim$ M [b]	Speed profile
LC-ISO [c]	L $\sim$ H [d]	M $\sim$ H [e]	Entry speed
SSR [f]	L $\sim$ M [g]	M $\sim$ H	Steering angle (according to radius of track), speed
SIS [h]	L $\sim$ M [g] $\sim$ H [e]	M $\sim$ H	Speed, amplitude and frequency of steering angle
SS [i]	L $\sim$ M, H [d]	M $\sim$ H	Steer angle amplitude, entry and final speed
Slalom18	L $\sim$ M $\sim$ H [e]	M $\sim$ H	Entry speed
Slalom36	L $\sim$ M $\sim$ H [e]	M $\sim$ H	Entry speed
CB [j]	H	M $\sim$ H	Entry speed, steering angle
CHB [k]	M $\sim$ H	H	Entry speed, steering angle
CBM [l]	M $\sim$ H	H	Entry speed, steering angle
BC [m]	H	M $\sim$ H [e]	Entry speed, deceleration
HSW [n]	L $\sim$ M	H	Entry speed, amplitude and period of steering angle

[a] B/A: Braking and acceleration
[b] steering involved on the low friction surface
[c] LC-ISO: ISO Lane Change
[d] braking involved on the low friction surface
[e] lose stability on the low friction surface
[f] SSR: Steady state radius cornering
[g] during acceleration
[h] SIS: Sine steering
[i] SS: Steering step
[j] CB: Cornering mild brake
[k] CHB: Cornering hard brake
[l] CBM: Cornering brake with friction split surface
[m] BC: Braking with minor steering
[n] HSW: High speed steering with sine dwell

The ranges of longitudinal and lateral slips in Table I are defined as low L, medium M and high H according to their excitation level (i.e. a typical low friction excitation level is defined as $|\alpha| < 0.05$[rad], $|s| < 0.02$) [9]. 129 simulation runs, in total, will be used as following: 17 B/A, 8 LC-ISO, 10 SSR, 10 SIS, 10 SS, 8 CB, 8 CHB, 22 CBM, 7 BC, 10 HSW, 9 Slalom 36, 10 Slalom 18m. White noise is added to simulated data to mimic the measurement error. But each noise is defined by different standard deviation for different variables due to difference in scale: 100N for forces in all directions; 10 % of the absolute value of longitudinal and lateral slips. To evaluate the generalization performance of the learned friction estimators and tire models, we split data from 129 runs into training and test datasets: training set includes 9 B/A, 13 CBM, 6 LC-ISO, 9 SIS, 8 Slalom 18, 7 Slalom 36, 5 SSR, 8 SS, test set includes some from the same maneuvers but different surfaces as training set - 8 B/A, 9 CBM, 5 SSR, 2 Slalom 36, 2 Slalom 18, 2 LC-ISO, 1 SIS, 2 SS, and 4 more extreme maneuvers - 8 test runs of CB, 7 BC, 10 HSW and CHB. Fig. 3 shows training and test data distributions in terms of longitudinal slip rate and lateral slip angle. Both datasets cover wide ranges of slips and two distributions are similar although they are generated from different maneuvers and road profiles .

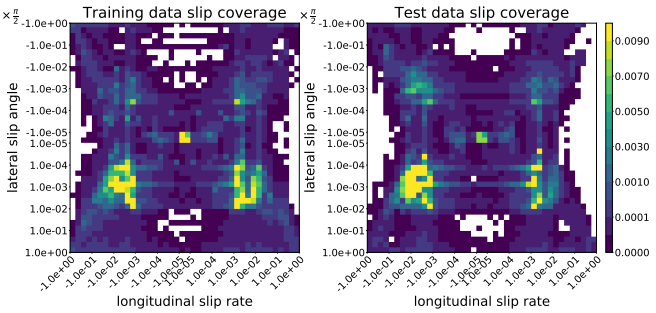

Fig. 3: Training and test data coverage comparison on longitudinal and lateral slip. Both x-axis and y-axis are specified in log scale.

2) Results and discussion: The MLP used for the friction estimator includes 3 layers of 20, 100, 2 of hidden units, and that of the tire model has layers of 20, 100 and 4 of hidden units[1]. Optimization is done by *Adam* [22] with default settings. Models are trained until convergence.

Qualitative evaluation on estimation accuracy and uncertainty

Fig. 4a shows average absolute errors of friction between estimated mean v_ϕ and ground truth μ_{GT} under different slips on the test data. In most of slip zones, average error is less than 0.1. It is clear that when either longitudinal or lateral slip enters into intermediate excitation levels ($|s| > 0.03$ or $|\alpha| > 0.03$[rad]), the estimation errors drop significantly. Thus, inference friction from multiple forces lows the requirement of tire excitation to reach adequate accuracy when either longitudinal or lateral direction to reach the intermediate levels, compared to the estimators that only utilize single force. As clearly observed from figure 1, at low slips, it is more difficult to differentiate forces under different friction levels so that friction information is harder to be extracted. It is expected that the average estimation error would increase with decreasing absolute longitudinal slip rates and lateral slip angles. However, estimation error is fairly low at extremely low slip range (under $\pm 10^{-4}$) in

[1] More implementation details are available at https://ssajj1212.github.io/publication/rfe_vi, including a detailed description of simulation data and setup in Carmaker.

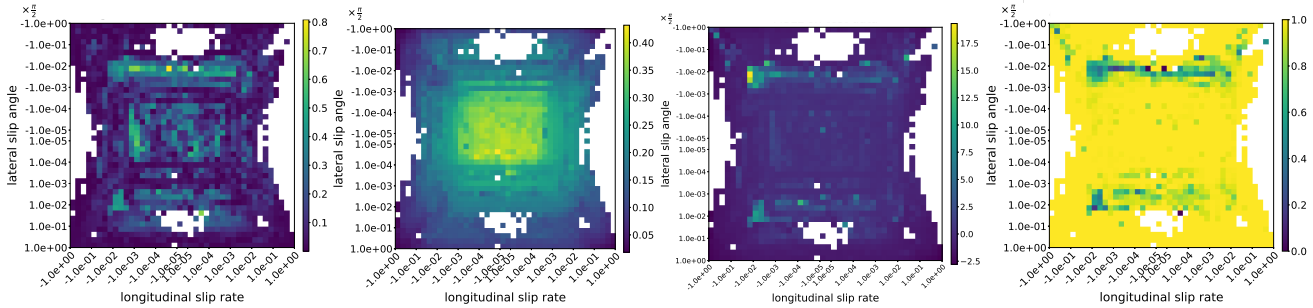

(a) Average estimation error (b) Average standard deviation (c) Mean standardized log loss (d) Ground truth within 95% confidence interval of estimation

Fig. 4: Performance of learned friction estimator on test data with regard of different longitudinal and lateral slip ranges.

TABLE II: Performance evaluation of friction inference and tire model compared to ground truth on test data

Ground truth within i	Friction inference μ		Longitudinal force F_x		Lateral force F_y	
confidence interval	Training	Test	Training	Test	Training	Test
68%	96.88 %	93.93 %	98.51 %	97.84 %	97.22 %	98.27 %
95%	98.97 %	96.66 %	99.30 %	98.91 %	98.72 %	99.12 %
99%	99.37 %	97.52 %	99.45 %	99.15 %	98.98 %	99.33 %

Fig. 4a. This phenomenon is mainly explained by the scarcity of data and unbalanced distribution of friction. A majority of data in this region come from high friction road profiles. The learned estimator succeeds to figure out to give biased but still accurate estimation. High estimation error regions concentrate at the neighborhood of lateral slip angles of about $\pm\frac{\pi}{2}\cdot 10^{-3}$[rad] where data comes from various friction profiles and maneuvers, but the excitation level is still too low to estimate accurately at the linear region. Since we specify approximation posterior as gaussian distribution, standard deviation directly reveals estimate uncertainty. Fig. 4b clearly shows that the uncertainty of estimates increases with decreasing tire excitation due to the difficulty of estimation in the linear region. Similarly, the standard deviation drops immediately when slip exits linear range in any direction.

Quantitative evaluation on estimate robustness

Robust uncertainty prediction prevents decision making algorithm from trusting less confident estimates since accepting overconfidently wrong estimates could potentially cause crashes especially when using point estimates by supervised learning methods. Although Fig. 4a and Fig. 4b show satisfying friction estimator qualitatively, quantitative evaluation could give us a better understanding on estimator performance. To quantify the performance of both learned friction estimator and probabilistic tire model, we evaluate the friction inference $q_\phi(\mu|\mathbf{F}, s, \alpha, F_z)$ on test data to actual friction by mean standardized log loss (MSLL) [23]. The metric is defined by considering the negative log probability of target μ_{GT} given the estimation mean $v_{\boldsymbol{\phi}}$ and standard deviation $\sigma_{\boldsymbol{\phi}}$:

$$-\log p(\mu_{GT}|v_\phi, \sigma_\phi) = \frac{1}{2}\log(2\pi\sigma_\phi^2) + \frac{(\mu_{GT} - v_\phi)^2}{2\sigma_\phi^2}, \quad (7)$$

where MSLL is computed by taking the mean of the negative log probability over test points. The lower the MSLL is, the better the estimation complies with its target. And it penalizes over-confidently wrong estimates especially when the target μ_{GT} does not fit in the estimated distribution $q_\phi(\mu|\mathbf{F}, s, \alpha, F_z)$, e.g. lying out of 68% confidence interval (or 1 standard deviation of estimate). Fig. 4c shows MSLL in each slip range on the test data. In most slip regions, MSLL remains less than 0 which illustrates that the target of friction is in the inference distribution and the estimation error is low. MSLLs are relatively large at few regions where longitudinal slip rates are around 0.02 and lateral slip angle close to $\frac{\pi}{2}\cdot 10^{-2}$[rad]. From previous qualitative analysis, in these regions, the average variance is comparatively low while the estimation error is high, thus the estimations are over-confidently wrong to make MSLLs large. Although estimation errors are large in low excitation regions as shown Fig.4a, the estimator succeeds to give under-confidence indications of estimations so that MSLLs are low.

Although MSLL is a well-behaved evaluation metric on robustness analysis, the averaged MSLL in each region could lead to under-estimation on friction estimator performance. The penalty of MSLL on overconfidently wrong estimations grows exponentially. Few poor estimates make MSLL declines substantially even though the estimator performs well on the majority of test samples. Therefore, we also report the percentage of data points having ground truth within 68%, 95% and 99% confidence intervals of the estimation distributions as an alternative metric. Table II shows the ratio of three confidence intervals on both training and test data. 93.93% of test data have true frictions within 68% confidence interval of estimates and only about 6% fail to give high-quality estimates. Comparing the estimation performance on training and test data under the same metrics, no substantial drop is observed despite the fact that training and test samples are from different maneuvers and road profiles. Therefore, the learned friction estimator is well generalized

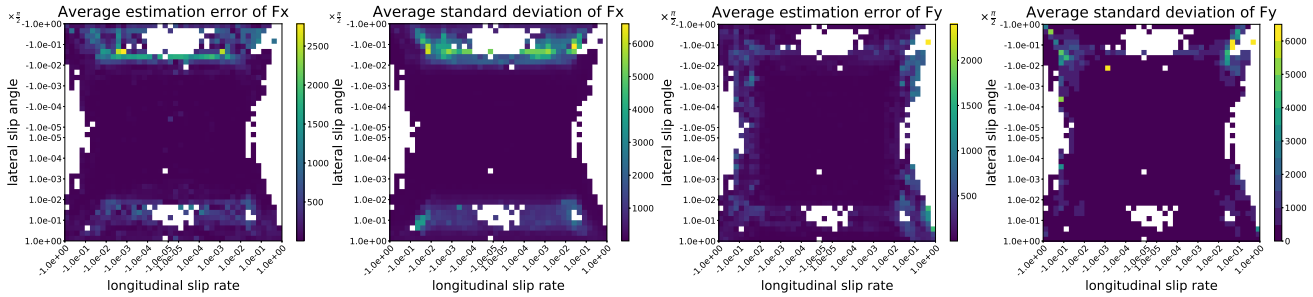

(a) longitudinal force performance

(b) lateral force performance

Fig. 5: Average error and standard deviation of probabilistic tire model on test data

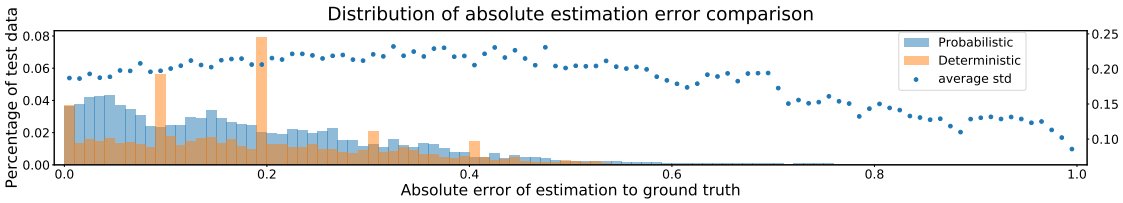

Fig. 6: Estimation error distribution comparison between probabilistic and deterministic friction estimator.

even to unseen scenarios. Fig. 4d shows the ratios of test data within the 95% confidence interval of estimations at different slips. The primary conclusion complies with that of MSLL: the friction estimator gives an accurate estimation mean with a reliable measure of confidence. However, at the peak regions of MSLLs in figure 4c, over 50% of test samples are still well estimated, albeit high MSLLs. Hence, large MSLL errors do not necessarily imply poor performance, if these errors only occur from few extremes. In addition, the regions of the worst performance according to 95% confidence interval are similar to the ones with high estimation error in figure 4a, except from the ones at low excitation levels. The correct indications of uncertainty at low excitation regions counteract for high estimation errors, thus the ratios of 95% confidence interval as well as MSLLs, are high instead.

Qualitative and Quantitative evaluation on learned tire model

The same evaluation metrics are applied to access the performance of the probabilistic tire model. Fig. 5a and Fig. 5b show average absolute errors and standard deviations of learned probabilistic tire model $p_{\boldsymbol{\theta}}(\mathbf{F}|\mu, s, \alpha, F_z)$ for longitudinal F_x and lateral force F_y in each slip zone respectively. Relative to the friction estimates, the normalized errors of force estimations are much smaller. At the linear range of the tire model, forces are similar at different friction levels, therefore the errors are relatively small in Fig. 5a and Fig. 5b. Conversely to friction estimator, higher error regions of force prediction are close to boundary of linear and non-linear regions in tire model. Except from these regions, standard deviations for both force estimates are rather low. The strong association between high estimation errors and high standard deviation, it is concluded that the standard deviation indicates uncertainty properly. The unsymmetrical estimation errors and standard deviations on positive and negative lateral slips are mainly caused by unbalanced simulations setup that more tests are anti-clockwise turnings than clockwise ones. Table II reports ratios of well behaved estimates under three different confidence intervals on both training and test data. For both longitudinal and lateral tire forces, about 98% of test points have true forces lying within the 68% confidence interval, and about 99% lying within the 95% confidence interval. The learned tire model is capable of predicting correct force estimates regardless of unbalanced and noisy data. It is likely that learned models, such as ours, provide an alternative to current state-of-the-art curve fitting techniques used in tire industry and to improve vehicle state estimation algorithms as in [20], [21].

Comparison to deterministic friction estimator

To further illustrate the advantage of probabilistic inference of friction over the point estimate by supervised learning, we compare a deterministic friction estimator to a probabilistic one using the same neural networks architecture, and learned from the same data. Given true friction, and noisy forces and slips, the deterministic model learns by minimizing the L2 loss as [20], [24]. Both deterministic and probabilistic friction estimators succeed to converge at similar training losses. Fig. 6 shows the distribution of absolute estimation error between the estimate from the deterministic model to ground truth and that of probabilistic model between the ground truth and estimated mean on test data. For both models, the majority of estimation error is under 0.2 and estimations with large errors are relatively rare. In addition, the probabilistic model outperforms the deterministic model when estimation errors are less than 0.1. Fig. 6 also shows the average standard deviation of the probabilistic estimation in each error range. The average standard deviation increases slightly with the increase in absolute error under 0.5. The estimation confidence from the probabilistic model can be used to prune poor estimates from further consideration,

whereas the deterministic model is not capable of distinguishing between poor estimates and better ones. In spite of the expected behavior of the probabilistic friction estimator on most test data, there is a small fraction of outliers for which both mean and standard deviation estimates are wrong. These outliers explains the decrease in standard deviation for errors larger than 0.5.

B. Field test

To verify the proposed method on real data, field tests were conducted to provide measurements from the test track located in Jokkmokk, Sweden. The test track offers homogeneous friction surfaces during test runs. High-quality force and moment measurements were collected by a Tire Test Trailer. Tests are on low-friction surfaces i.e. scraped ice, ice, soft packed snow, water and etc, corresponding to different friction coefficients of surfaces. Due to the limitation of the Tire Test Trailer, combined slip tests are only executed under fixed lateral slip angles with varying longitudinal slip rates and only under negative longitudinal slips. Fig. 7 shows both training and test data distributions on longitudinal slip rates and lateral slip angles. Data concentrates on low longitudinal slip rates and lateral slip angles, and is distributed at discrete lateral slip angles except when the longitudinal slip rate is 0.

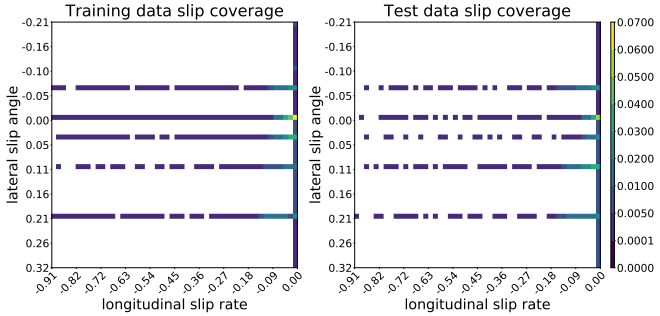

Fig. 7: Data distribution of field test data regarding longitudinal slip rate and lateral slip angle.

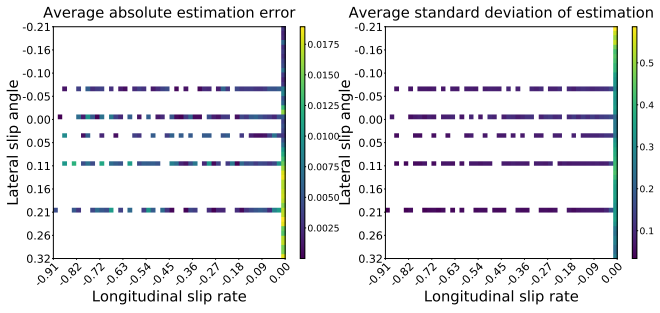

Fig. 8: Evaluation of friction estimation regarding averaged estimation error and standard deviation on different longitudinal slip rate and lateral slip angle range.

Evaluation on friction estimator

Similar to simulation, we only utilize longitudinal and lateral forces as the force vector $\mathbf{F}$, longitudinal slip rate s, lateral slip angle α, and nominal force F_z in training. Fig. 8 shows average absolute estimation error and standard deviation of learned friction estimator. The average error in friction estimates, the difference between estimated mean and ground truth, is under 0.02, and large longitudinal slip rates lead to small estimation errors. Since data collected from the field tests are mainly from low to medium friction surfaces, the estimation is easier, therefore, more accurate for the field tests compared to simulation. Errors decrease rapidly when either longitudinal or lateral slip leaves linear region of tire model in the field test as simulation data. However, errors grow slightly with increasing lateral slip angles at 0 longitudinal slip rate for the field test data. The main cause of this is insufficient data at high excitation of lateral slip, as shown in figure 7. Regarding quantitative evaluation, MSLLs are under 0 in all regions. The learned friction estimator from real tire measurement is able to provide estimates with limited errors and reasonable uncertainty estimates.

Evaluation on probabilistic tire model

To evaluate the learned tire model, we use tests on a scraped ice surface which has a friction coefficient of about 0.42, under three different vertical load levels of about 3142N, 6427N, and 9536N. Fig. 9 shows the mean of longitudinal and lateral forces of the learned tire model at each nominal force respectively comparing to actual data points. It is clearly shown that the learned tire model performs well in a wide range of longitudinal and lateral slips at each nominal force. The combined slip effect is indeed learned for both forces, which means that correction of combined slip by analytical or empirical model like *Magic Formula* could be revealed from data. Although slips in both longitudinal and lateral directions are not evenly distributed and discrete, the learned tire model is smooth and captures the combined slip characteristics of the tire model under different nominal forces.

V. Conclusion

The proposed amortized variational friction estimator facilitates the approximation of exact Bayesian inference to facilitate uncertainty prediction of estimates without compromising the flexibility of tire models. From simulation and field test experiments, the learned friction estimator is proved to give accurate friction estimation in the wide range of excitation levels of tire, on various unseen friction surfaces and maneuvers. The required excitation levels for accurate estimates is lowered compared to common estimation algorithm. Measures of uncertainty is robust enough to provide correct indications of estimate confidence to enable ADAS or Autonomous driving functions to be activated accordingly. Learning from data leads more accurate modeling and minimizes labors in manually design and tune estimation algorithms for different tires. Meanwhile, proposed method could learn tire model without prior knowledge. The learned model well reflects tire characteristics in both simulation and field test, which possibly helps to reveal more tire

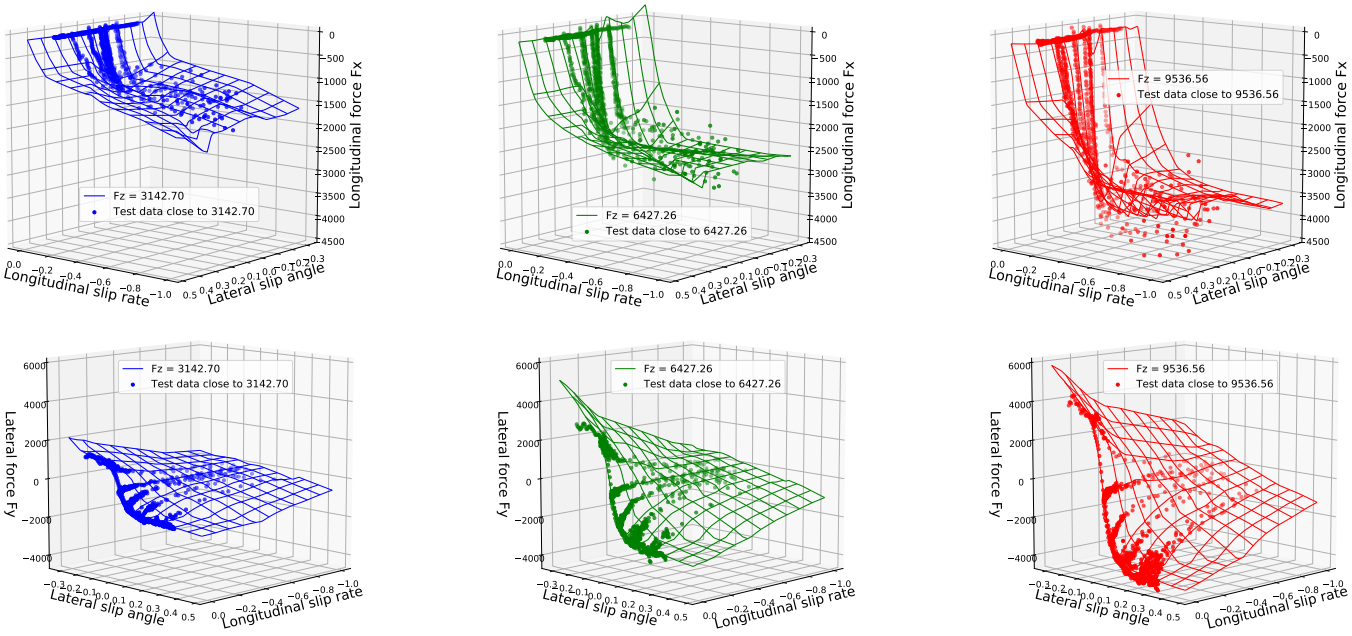

(a) Nominal load at 3142.70N (b) Nominal load at 6427.26N (c) Nominal load at 9536.56N

Fig. 9: Longitudinal and lateral tire forces of learned tire model given various nominal loads compared to test data with the same load $\pm 1000N$ on a surface with friction coefficient of about 0.42.

characteristics and provides more realistic tire behaviors in future simulations.

Acknowledgements

We would like to thank Niklas Ohlsson, Shenhai Ran, Alejandro Gonzalez for advice in simulation and field test data, thank Mats Jonasson, Bengt Jacobsson for insightful discussion in vehicle dynamics. This work is supported by the Wallenberg AI, Autonomous Systems and Software Program (WASP).

References

[1] C. S. Ahn, "Robust estimation of road friction coefficient for vehicle active safety systems." Ph.D. dissertation, 2011.

[2] S. Moon, I. Moon, and K. Yi, "Design, tuning, and evaluation of a full-range adaptive cruise control system with collision avoidance," *Control Engineering Practice*, vol. 17, no. 4, pp. 442–455, 2009.

[3] S. Koskinen, "Sensor data fusion based estimation of tyre-road friction to enhance collision avoidance," 2010.

[4] D. Piyabongkarn, R. Rajamani, J. A. Grogg, and J. Y. Lew, "Development and experimental evaluation of a slip angle estimator for vehicle stability control," *IEEE Trans. on control systems technology*, vol. 17, no. 1, pp. 78–88, 2008.

[5] F. Gustafsson, "Slip-based tire-road friction estimation," *Automatica*, vol. 33, no. 6, pp. 1087–1099, 1997.

[6] L. R. Ray, "Nonlinear tire force estimation and road friction identification: Simulation and experiments," *Automatica*, vol. 33, no. 10, pp. 1819–1833, 1997.

[7] J. Svendenius, "Tire modeling and friction estimation," Ph.D. dissertation, Automatic Control Dept., Lund Univ., Lund, Sweden, 2007.

[8] C. Ahn, H. Peng, and H. E. Tseng, "Robust estimation of road friction coefficient using lateral and longitudinal vehicle dynamics," *Vehicle System Dynamics*, vol. 50, no. 6, pp. 961–985, 2012.

[9] M. Acosta, S. Kanarachos, and M. Blundell, "Road friction virtual sensing: a review of estimation techniques with emphasis on low excitation approaches," *Applied Sciences*, vol. 7, no. 12, p. 1230, 2017.

[10] U. Eichhorn and J. Roth, "Prediction and monitoring of tyre/road friction," in *Proc. FISITA, London*, 1992.

[11] P. Boyraz and D. Dogan, "Intelligent traction control in electric vehicles using an acoustic approach for online estimation of road-tire friction," in *2013 IEEE Intelligent Vehicles Symposium (IV)*. IEEE, 2013, pp. 1336–1343.

[12] A. Jonnarth, "Camera-based friction estimation with deep convolutional neural networks," Master's thesis, 2018.

[13] G. Panahandeh, E. Ek, and N. Mohammadiha, "Road friction estimation for connected vehicles using supervised machine learning," in *IEEE Intelligent Vehicles Symposium, IV 2017, Los Angeles, CA, USA, June 11-14, 2017*. IEEE, 2017, pp. 1262–1267.

[14] H. B. Pacejka, *Tire and vehicle dynamics*. Elsevier, 2012.

[15] I. Besselink, A. Schmeitz, and H. B. Pacejka, "An improved magic formula/swift tyre model that can handle inflation pressure changes," *Vehicle System Dynamics*, vol. 48, no. S1, pp. 337–352, 2010.

[16] E. B. Hans B. Pacejka, "The magic formula tyre model," *Vehicle system dynamics*, vol. 21, no. S1, pp. 1–18, 1992.

[17] D. Koller and N. Friedman, *Probabilistic graphical models: principles and techniques*. MIT press, 2009.

[18] D. P. Kingma, S. Mohamed, D. J. Rezende, and M. Welling, "Semi-supervised learning with deep generative models," in *Advances in neural information processing systems*, 2014, pp. 3581–3589.

[19] D. P. Kingma and M. Welling, "Auto-encoding variational bayes," in *2nd International Conference on Learning Representations, ICLR 2014, Banff, AB, Canada, April 14-16, 2014, Conference Track Proceedings*, 2014.

[20] A. Zareian, S. Azadi, and R. Kazemi, "Estimation of road friction coefficient using extended kalman filter, recursive least square, and neural network," *Proceedings of the Institution of Mechanical Engineers, Part K: Journal of Multi-body Dynamics*, vol. 230, no. 1, pp. 52–68, 2016.

[21] M. Acosta and S. Kanarachos, "Tire lateral force estimation and grip potential identification using neural networks, extended kalman filter, and recursive least squares," *Neural Computing and Applications*, vol. 30, no. 11, pp. 3445–3465, 2018.

[22] D. P. Kingma and J. Ba, "Adam: A method for stochastic optimization," in *3rd International Conference on Learning Representations, ICLR 2015, San Diego, CA, USA, May 7-9, 2015, Conference Track Proceedings*, Y. Bengio and Y. LeCun, Eds., 2015.

[23] C. E. Rasmussen and C. K. Williams, *Gaussian processes for machine learning*. MIT press, 2006.

[24] J. Matusko, I. Petrović, and N. Perić, "Neural network based tire/road friction force estimation," *Engineering Applications of Artificial Intelligence*, vol. 21, no. 3, pp. 442–456, 2008.